Focus on Fluids journals.cambridge.org/focus

Slickwater hydraulic fracturing of shales

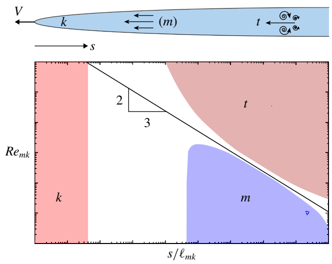

Emmanuel Detournay†

Department of Civil, Environmental, and Geo- Engineering, University of Minnesota, Minneapolis, MN 55455, USA

Stimulation of gas or oil shales by hydraulic fracturing requires injecting water at a very high rate into kilometre-long boreholes, in order to induce sufficient fracture width to place the proppant. Since such high rate of injection implies flow in the turbulent regime, heavy-molecular-weight polymers are added to water to reduce drag and thus drastically lessen the energy required for pumping. Lecampion & Zia (*J. Fluid Mech.*, vol. 880, 2019, pp. 514–550) explore via modelling how the rheology of slickwater – water with a small amount of drag-reducing agents – affects the propagation of a hydraulic fracture. Theoretical models in combination with scaling arguments and numerical simulations indicate that flow in a radial fracture is inherently laminar, with the turbulent regime restricted at most to the first few minutes of injection, for plausible values of rock and fluid parameters and the injection rate.

Key words: lubrication theory, rheology, turbulent transition

1. Introduction

Hydraulic fracturing is one of the essential technologies behind the gas shale revolution, which started in the early years of this century. Indeed, effective production of hydrocarbons from low-porosity shale deposits relies on placing, in successive stages, tens to hundreds of hydraulic fractures in the horizontal section of each borehole (Patterson, Yu & Wu 2018). This hydraulic fracturing treatment requires, however, to inject water at a very high rate from the surface into kilometre-long boreholes, in order to induce sufficient fracture width to place the proppant. Furthermore, the treatment design involves the simultaneous propagation of several fractures from perforation clusters, thus imposing further requirement for large injection rate. To reduce the energy demand and keep the operation economically viable, heavy-molecular-weight polymers are added to the water to substantially reduce drag in the turbulent regime. The effect of these drag-reducing agents saturates at relatively low polymer concentration, leading to the emergence of a maximum drag reduction (MDR) asymptote when the Reynolds number *Re* is approximately 10^3.

† Email address for correspondence: detou001@umn.edu

J. Fluid Mech. (2020), *vol.* 886, F1.
Published by Cambridge University Press
doi:10.1017/jfm.2019.1023

The main issue considered by Lecampion & Zia (2019), henceforth LZ, is the influence on the propagation of a radial hydraulic fracture of the drag-reduction agents in combination with the large injection rate. They tackle this question through a theoretical effort that involves the development of models applicable to slickwater fracturing. Their analysis concludes, however, that flow in the fracture is inherently laminar with the turbulent regime restricted at most to the first few minutes of injection.

2. Overview

2.1. *Mathematical model*

Two fundamental equations govern the fracture aperture w and the fluid pressure p: a non-local elasticity equation and the nonlinear Reynolds lubrication equation. Together with the boundary and initial conditions and the propagation criterion, they provide a complete formulation of the evolution problem (Detournay 2016). Two regimes of flow are considered by LZ for slickwater hydraulic fracturing: the viscous laminar regime with friction factor $f \sim Re^{-1}$ and the turbulent MDR regime for which $f \sim Re^{-0.7}$. The mathematical model depends on Young's modulus E, Poisson's ratio ν and toughness K_{Ic} for the rock, and viscosity μ, density ρ and index n for the fluid, where $n = 1$ for laminar flow and $n = 0.7$ in the turbulent MDR regime, as well as on the injection rate Q. However, to avoid carrying numerical factors in the definitions of the length and time scales below, the following alternative material parameters are introduced:

$$E' = \frac{E}{1-\nu^2}, \quad K' = 4\left(\frac{2}{\pi}\right)^{1/2} K_{Ic}, \quad \mu' = 12\mu, \quad \rho' = 0.0106\rho. \qquad (2.1a\text{–}d)$$

2.2. *Tip asymptotic solution*

Asymptotics of the solution near the advancing tip of a hydraulic fracture have the structure of a travelling wave. Hence, near the crack front, the dependence of the solution on position and time reduces to a dependence of the asymptotic fields on the distance from the crack front, with the current local-front velocity V acting as a time-dependent parameter. Asymptotic solutions were initially restricted to situations involving the laminar flow of a Newtonian fluid, one-dimensional leak-off and linear elastic fracture mechanics (Garagash, Detournay & Adachi 2011); they have recently been extended to include shear-thinning fluid (Dontsov & Kresse 2018; Moukhtari & Lecampion 2018) and turbulent flow (Dontsov 2016).

In the spirit of these solutions, LZ construct a multiscale tip asymptote applicable to slickwater hydraulic fracturing. This solution captures three distinct regimes of energy dissipation: (i) close to the tip, a region dominated by dissipation in the creation of new solid surfaces; (ii) an intermediate region dominated by viscous laminar dissipation; and (iii) far from the tip, a region dominated by turbulent MDR flow. The solution is characterized by two independent length scales, ℓ_{mk} and ℓ_{tm}, given by

$$\ell_{mk} = \frac{K'^6}{E'^4 \mu'^2 V^2}, \quad \ell_{tm} = \frac{E'^{1/2}\mu'}{\rho'^{3/2} V^2}, \quad \ell_{tk} = \ell_{mk}^{27/39} \ell_{tm}^{12/39}, \quad Re_{mk} = Re_c \left(\frac{\ell_{mk}}{\ell_{tm}}\right)^{2/3}, \quad (2.2a\text{–}d)$$

where ℓ_{tk} is a third length scale and Re_{mk} is a characteristic Reynolds number, which both depend on ℓ_{mk} and ℓ_{tm} only, and $Re_c \simeq 1133$.

https://doi.org/10.1017/jfm.2019.1023 Published online by Cambridge University Press

The crack aperture, in each of the three regions dominated by a particular dissipation, varies as a power law of distance s from the tip: a near-tip toughness k-asymptote with $\hat{w} \sim s^{1/2}$, an intermediate viscous laminar m-asymptote with $\hat{w} \sim s^{2/3}$, and a far-tip turbulent MDR t-asymptote with $\hat{w} \sim s^{20/27}$. Length scales ℓ_{mk} and ℓ_{tm} are proportional to the bounds of the intermediate m-asymptote region, which correspond approximately to $10^{-1}\ell_{mk} < s < \ell_{tm}$. Also the k-asymptote exists within distances from the tip less than approximately $10^{-5}\ell_{mk}$. However, as suggested by the above expression for Re_{mk}, the intermediate asymptote region shrinks with increasing Re_{mk} to eventually disappear when $Re_{mk} \sim Re_c$. Thus, for large characteristic Reynolds numbers, there are only two power-law regions, the k-asymptote at $s \lesssim 10^{-5}\ell_{mk}$ and the t-asymptote at $s \gtrsim \ell_{tk}$.

The tip length scales ℓ_{mk}, ℓ_{tm} and ℓ_{tk} legislate the nature of dissipation near the front of a finite hydraulic fracture and control how the dominant mode of dissipation changes with time. Let ℓ denotes the distance from the front over which the autonomous tip solution is applicable; for a penny-shaped fracture, ℓ is a constant fraction, say 10 %, of the fracture radius R. The key point to recognize is that all the tip length scales defined above increase with time, relative to ℓ.

At small time, the tip region is effectively fully described by the t-asymptote. Under these conditions, the global solution is completely shielded from both the k- and the m-asymptotes, which exist in a tiny region at the tip. However, as time progresses, the sizes of the tip length scales ℓ_{mk}, ℓ_{tm} and ℓ_{tk} increase relative to ℓ, causing the disappearance of the turbulent MDR asymptote from the tip region of the finite fracture and the progressive emergence of the m-asymptote. As long as the k-asymptote region is small compared to ℓ, the global solution does not depend on the toughness. However, further passing of time leads to the growth of the k-asymptotic region relative to ℓ, at the expense of the m-asymptote. Thus at large time, the tip region of the finite fracture is dominated by the k-asymptote, with the consequence that the fracture propagates in the toughness-dominated regime. If Re_{mk} is larger than Re_c, the intermediate viscous laminar regime is bypassed, with the t-asymptote dominating the tip region at small time and the k-asymptote at large time. The figure alongside the title illustrates the region of dominance of each asymptote.

2.3. *Penny-shaped fracture*

The above classification of the dominance of a particular mode of energy dissipation is based on contrasting length scales ℓ_{mk}, ℓ_{tm} and ℓ_{tk} with the size ℓ of the tip region. However, it can be recast in terms of time for a radial hydraulic fracture propagating under constant injection rate, through the introduction of time scales expressing transition between regimes of propagation. These time scales are linked to the existence of three similarity solutions for slickwater fracturing, all characterized by a power-law dependence of the fracture radius R on time. In addition to two known similarity solutions (Savitski & Detournay 2002), where energy is dissipated exclusively either in viscous laminar flow (M-solution with $R \sim t^{4/9}$) or in the creation of fracture surfaces (K-solution with $R \sim t^{2/5}$), LZ demonstrated the existence of a third similarity solution (T-solution with $R \sim t^{40/87}$) with all the dissipation taking place in the fluid in the turbulent MDR regime. Each similarity solution is characterized by a dominant tip asymptote; for example, the tip asymptote viewed at the fracture scale is the t-asymptote for the T-solution.

Transition time scales are deduced naturally from the similarity solutions. Three such scales, T_{tk}, T_{tm} and T_{mk}, can be determined, but only two are independent:

$$T_{tk} \sim \left(\frac{E'^{124} \mu'^{35} \rho'^{15} Q^{39}}{K'^{174}} \right)^{1/26}, \quad T_{tm} \sim \left(\frac{\rho'^9 Q^6}{E' \mu'^8} \right)^{1/4}, \quad T_{mk} \sim \left(\frac{T_{tk}^{39}}{T_{tm}^{10}} \right)^{1/29}, \quad \varphi = \frac{T_{tm}}{T_{mk}}. \qquad (2.3a\text{–}d)$$

When measuring time relative to these time scales, it can then be demonstrated that (i) the T-solution is the small-time asymptote ($t/T_{tm} \ll 1$ and $t/T_{mk} \ll 1$), (ii) the K-solution is the large-time asymptote ($t/T_{mk} \gg 1$), and (iii) the M-solution is an intermediate-time asymptote when $t/T_{tm} \gg 1$ and $t/T_{mk} \ll 1$, and which exists provided that there is separation of the two time scales, i.e. if $\varphi = T_{tm}/T_{mk} \ll 1$.

Numerical simulations confirm that the time scales derived from a scaling analysis provide an adequate measure of the transition time between regimes. The results of two simulations are reported: one with $\varphi \simeq 10^{-3}$, which confirms the transition between the T- and the M-solutions; the other with $\varphi \simeq 4$, which describes the transition between the T- and the K-solutions. These simulations and the time scales indicate that, for plausible values of the rock and fluid parameters and of the injection rate, the turbulent regime is restricted at most to the first few minutes of injection.

3. Future

Advances in theoretical predictions must necessarily rely on further understanding of the rheology of slickwater. As noted by the authors, the addition of heavy-molecular-weight polymers to water increases the viscosity of the fluid, but also introduces a degree of shear thinning and viscoelasticity. While the increase of viscosity is expected to further reduce or even eliminate the turbulent flow regime, the breaking of the polymer chains caused by high downhole temperature or high shear rate could degrade the fluid and thus reduce its capacity to lower drag in the turbulent flow regime. These effects, as well as the progressive damage of the rock at the crack tip, should be considered in future models of slickwater hydraulic fracturing.

References

DETOURNAY, E. 2016 Mechanics of hydraulic fractures. *Annu. Rev. Fluid Mech.* **48**, 311–339.

DONTSOV, E. V. 2016 Tip region of a hydraulic fracture driven by a laminar-to-turbulent fluid flow. *J. Fluid Mech.* **797**, R2.

DONTSOV, E. V. & KRESSE, O. 2018 A semi-infinite hydraulic fracture with leak-off driven by a power-law fluid. *J. Fluid Mech.* **837**, 210–229.

GARAGASH, D. I., DETOURNAY, E. & ADACHI, J. I. 2011 Multiscale tip asymptotics in hydraulic fracture with leak-off. *J. Fluid Mech.* **669**, 260–297.

LECAMPION, B. & ZIA, H. 2019 Slickwater hydraulic fracture propagation: near-tip and radial geometry solutions. *J. Fluid Mech.* **880**, 514–550.

MOUKHTARI, F.-E. & LECAMPION, B. 2018 A semi-infinite hydraulic fracture driven by a shear-thinning fluid. *J. Fluid Mech.* **838**, 573–605.

PATTERSON, R., YU, W. & WU, K. 2018 Integration of microseismic data, completion data, and production data to characterize fracture geometry in the permian basin. *J. Natural Gas Sci. Engng* **56**, 62–71.

SAVITSKI, A. A. & DETOURNAY, E. 2002 Propagation of a fluid-driven penny-shaped fracture in an impermeable rock: asymptotic solutions. *Intl J. Solids Struct.* **39** (26), 6311–6337.